Inorg. Chem. **2003**, *42*, 8320–8327

A Novel Layered Niobium Oxychloride Compound Based on Nb_2 Pairs and Nb_6 Octahedral Clusters: Synthesis and Crystal and Electronic Structures of $Nb_{10}Cl_{16}O_7$

Stéphane Cordier,*,† Fakhili Gulo,‡ Thierry Roisnel,† Régis Gautier,§ Boris le Guennic,† Jean François Halet,† and Christiane Perrin†

Laboratoire de Chimie du Solide et Inorganique Moléculaire (LCSIM), UMR 6511 CNRS-Université de Rennes 1, Institut de Chimie de Rennes, Avenue du Général Leclerc, 35042 Rennes Cedex, France, and Laboratoire de Physicochimie, UPRES 1795, Ecole Nationale Supérieure de Chimie de Rennes, Institut de Chimie de Rennes, Campus de Beaulieu, 35700 Rennes, France

Received September 17, 2003

The synthesis, single crystal structure determination, and electronic structure of $Nb_{10}Cl_{16}O_7$, the first Nb_6 oxychloride stabilized without countercation, are reported in this work. The crystal structure is very original since it consists of layers built up from both Nb_6 octahedral clusters and Nb_2 pairs. The $Nb_6O^i{}_6Cl^i{}_6Cl^a{}_6$ and $Nb_2(\mu_2\text{-}Cl)_2Cl_4O_4$ units form $[Nb_6Cl^i{}_6O^i{}_4O^{i-i}{}_{2/2}Cl^{a-a}{}_{4/2}Cl^a{}_2]_\infty$ infinite chains and $[\{Nb_2(\mu_2\text{-}Cl)_2O_{2/2}Cl_{4/2}O_2\}_2]_\infty$ double chains, respectively, that are interconnected by shared oxygen and chlorine ligands leading to layers. The cohesion of the three-dimensional structure (3D) is ensured by van der Waals contacts between layers that are randomly stacked along the [011] direction. Structural correlations between $Nb_{10}Cl_{16}O_7$ and related Nb_6 cluster oxyhalides, as well as $NbOCl_2$ and $NbCl_4$ containing Nb_2 pairs, are discussed. DFT results show that among the 20 valence electrons involved in the metal–metal bonding states, 14 electrons belong to the octahedral $Nb_6Cl^i{}_6O^i{}_6Cl^a{}_6$ unit whereas the 6 others (i.e., 1.5 per Nb atom) participate in the bonding in the distorted $[\{Nb_2(\mu_2\text{-}Cl)_2O_{2/2}Cl_{4/2}O_2\}_2]_\infty$ double chains.

Introduction

The $[(Nb_6L^i{}_{12})L_6{}^a]^{n-}$ cluster unit (L = F, Cl, Br, O) constitutes the basic building block of niobium octahedral cluster chemistry.[1] The Nb_6 cluster, edge-bridged by 12 μ_2 inner ligands (L^i), is stabilized by six additional ligands in terminal position (L^a) (^{a} = apical, ^{i} = inner according to the Schäfer and Schnering notation).[2] In halides, the unit interconnection via shared apical ligand (L^{a-a}) leads to one-, two-, or three-dimensional unit networks as observed, for instance, in $Cs_2Nb_6Br_5F_{12}$ ($Cs_2Nb_6Br^i{}_5F^i{}_7F^{a-a}{}_{2/2}F^a{}_4$),[3] $Li_2Nb_6Cl_{16}$ ($Li_2Nb_6Cl^i{}_{12}Cl^{a-a}{}_{4/2}Cl^a{}_2$),[4] and Nb_6F_{15} ($Nb_6F^i{}_{12}F^{a-a}{}_{6/2}$),[5] respectively. On the other hand, in the case of oxides, the $Nb_6O^i{}_{12}O^a{}_6$ unit condensation occurs not only through O^{a-a} but also through O^{i-a} and O^{i-i} bridges.[6] In contrast to the molecular character of the Nb_6 cluster halides, the strong interactions between the $Nb_6O^i{}_{12}O^a{}_6$ units in niobium oxides frequently lead to band structures.[7] The ultimate condensation of the $Nb_6O^i{}_{12}O^a{}_6$ units, observed in the NbO ($Nb_{6/2}O^{i-i-i-i}{}_{12/4}$) binary compound, induces transport properties with a superconducting transition at low temperature.[8] The physical properties of the cluster compounds are related to the strength of interaction between cluster units and the number of electrons available for metal−metal bonding, the so-called valence electron count (VEC). Hitherto, for pure oxides and

* To whom correspondence should be addressed. E-mail: stephane.cordier@univ-rennes1.fr.
† CNRS-Université de Rennes 1.
‡ Permanent address: FKIP Universitas Sriwijaya, Kampus-Inderalaya, Palembang, Indonesia.
§ Ecole Nationale Supérieure de Chimie de Rennes.

(1) (a) Perrin, C.; Cordier, S.; Ihmaïne, S.; Sergent, M. *J. Alloys Compd.* **1995**, *229*, 125. (b) Köhler, J.; Svensson, G.; Simon, A. *Angew. Chem., Int. Ed. Engl.* **1992**, *31* (1), 1437. (c) Cordier, S.; Hernandez, O.; Perrin, C. *J. Fluorine Chem.* **2001**, *107*, 205.
(2) Schäfer, H.; von Schnering, H.-G. *Angew. Chem.* **1964**, *76*, 833.
(3) Cordier, S.; Hernandez, O.; Perrin, C. *J. Solid State Chem.* **2002**, *163*, 319.
(4) Bajan, B.; Meyer, H.-J. *Z. Anorg. Allg. Chem.* **1997**, *623*, 791.
(5) Schäfer, H.; Schnering, H. G.; Niehues, K. J.; Nieder-Varenholz, H. G. *J. Less-Common Met.* **1965**, *9*, 95.
(6) Svensson, G.; Köhler, J.; Simon, A. *Metal Clusters in Chemistry*; Braunstein, P., Oro, L. A., Raithby, P. R., Eds.; Wiley-VCH: Weinheim, 1999; p 1485.
(7) Vajenine, G. V.; Simon, A. *Inorg. Chem.* **1999**, *38*, 3463.
(8) Brauer, G. *Z. Anorg. Allg. Chem.* **1941**, *248*, 1.

10.1021/ic0350990 CCC: $25.00
Published on Web 11/01/2003

halides containing $[(M_6L^i_{12})L^a_6]^{n-}$ units, it has been experimentally found that the VEC lies between 13 and 16 electrons per Nb_6 cluster.

The discovery of the first Nb_6 oxyhalide by some of us, namely $ScNb_6Cl_{13}O_3$,[9] opened the field of a new class of octahedral niobium cluster compounds. The ordered oxygen/halogen distribution within the $Nb_6X_{18-x}O_x$ unit (X = Cl or Br) leads to great distortions of the cluster and to various electronic counts (13−16) in relation to the discrepancy between the ionic radii and between the charges of oxygen and chlorine or bromine atoms.[10] Furthermore, the condensation of oxychloride units through O^{i-a} and O^{a-i} bridges allowed us to stabilize low-dimensional structures such as $Na_{0.21}Nb_6Cl_{10.5}O_3$, for instance, which exhibits a graphite-like topology[11] or $CsNb_6Cl_{12}O_2$ which is built from chains of cluster units.[12] Over the past few years, numerous niobium oxychlorides based on $(Nb_6Cl_{12-x}O_x)^{n+}$ cluster cores with $x = 1-6$ have been synthesized by solid state chemistry routes and structurally characterized.[11−13] This has been recently extended to solution chemistry yielding $[(Nb_6Cl^i_{12-x}O^i_x)(CN)^a_6]^{n-}$ anions[14,15] that could serve as a virtual library for the construction of polymeric cluster solids with different dimensionalities as observed in rhenium cluster chemistry, for instance.[16]

We report here the synthesis, single crystal structure determination and electronic structure of $Nb_{10}Cl_{16}O_7$, the first oxychloride compound containing octahedral Nb_6 clusters stabilized without countercation. The structure of the title compound consists of layers built up from $Nb_6O^i_6Cl^i_6Cl^a_6$ and $Nb_2(\mu_2\text{-}Cl)_2Cl_4O_4$ units which form, respectively, $[Nb_6Cl^i_6O^i_4O^{i-i}_{2/2}Cl^{a-a}_{4/2}Cl^a_2]_\infty$ infinite chains and $[\{Nb_2(\mu_2\text{-}Cl)_2O_{2/2}Cl_{4/2}O_2\}_2]_\infty$ double chains interconnected by shared oxygen and chlorine ligands. The cohesion of the three-dimensional structure (3D) is ensured by van der Waals contacts between layers. The crystal structure evidences a disordered stacking of layers. Structural and electronic correlations between $Nb_{10}Cl_{16}O_7$ and related Nb_6 cluster oxyhalides, as well as $NbOCl_2$ and $NbCl_4$ containing Nb_2 pairs, are discussed.

Experimental Section

Synthesis. A starting mixture (3.5 g) of CsCl (Prolabo), Nb (Ventron m2N8), Nb_2O_5 (Merck, Optipur), and $NbCl_5$ (Alfa 99.9%) (ratio 5/15/2/11) was handled, ground under inert atmosphere, and introduced in a quartz tube (length 15 cm) subsequently sealed under vacuum. This tube was then placed in a horizontal furnace, and the temperature was increased within one week in order to obtain a temperature gradient (620−700 °C). After two months of reaction, the tube was cooled to room temperature within two weeks. Fibrous crystals of $Nb_{10}Cl_{16}O_7$ grew on the upper side of the tube corresponding to the 640/650 °C region. A preliminary chemical analysis by energy dispersive spectrometry (EDS), using a scanning electron microscope JEOL JSM 6400 equipped with a microprobe EDS OXFORD LINK ISIS (Centre de Microscopie Electronique et de Microanalyse de l'Université de Rennes 1, France), showed that all the single crystals contained Nb, Cl, and O elements with the following atomic percentage: Nb/Cl/O 30.9/44.6/24.5 (calculated atomic percentage composition for $Nb_{10}Cl_{16}O_7$: 30.3/48.5/21.2). The cesium element was not detected in any crystals. Many attempts were performed to isolate single crystals for structural investigation. Indeed, they were very brittle under manipulation due to their layered structure (see a following description). Finally, small plate-shaped single crystals of the title compound, suitable for X-ray diffraction studies, were carefully handled, selected, and held with grease on a capillary tube.

Further attempts to obtain $Nb_{10}Cl_{16}O_7$ from stoichiometric amounts of Nb, Nb_2O_5, and $NbCl_5$ gave a black microcrystalline compound with a good yield. Only small amounts of $NbOCl_2$[17] were observed in the X-ray powder pattern. Despite many experiments, no single crystal suitable for structural determination has been found from these direct preparations.

Data Collection and Structural Refinement. The selected single crystals were mounted on a Nonius KappaCCD X-ray area-detector diffractometer with Mo Kα radiation (λ = 0.71073 Å) (Centre de Diffractométrie de l'Université de Rennes 1, France). Diffraction intensities were collected for one of these single crystals at room temperature. Once the data processing was performed by the KappaCCD analysis software,[18] the parameters of the centered monoclinic unit cell were refined as follows: a = 17.6467(8) Å, b = 3.2638(2) Å, c = 12.8928(6) Å, β = 121.243(2)°, V = 634.88(6) Å^3. A first analysis revealed that all the selected crystals exhibited the same cell parameters within the standard uncertainties (su's) with a *C*-centered lattice. The structure was first solved in the *C*2/*m* space group by direct methods (SIR-97 program[19]) combined with Fourier difference syntheses and refined against F^2 (SHELXL-97 program[20]). The refinements were successfully carried out in this unit cell and allowed to generate a first disordered structural model (R1 = 0.0318, wR2 = 0.0940, $\Delta\rho_{min}$ = −0.942 e$^-$/Å^3, $\Delta\rho_{max}$ = 0.795 e$^-$/Å^3; 855 independent reflections for 62 parameters and 756 reflections with $I > 2\sigma(I)$). This structural model will be briefly described in this paper. Complete data (CIF file) are available in Supporting Informations. This first result allowed us to conclude that the structure of the layered $Nb_{10}Cl_{16}O_7$ oxychloride consists of $Nb_6Cl^i_6O_6{}^iCl^a_6$ units sharing two O^i and four Cl^a ligands with adjacent units to form infinite $[Nb_6Cl^i_6O^i_4O^{i-i}_{2/2}Cl^{a-a}_{4/2}Cl^a_2]_\infty$ chains. The presence of $Nb_2(\mu_2\text{-}Cl^i)_2Cl^a_4O^a_4$ units

(9) Cordier, S.; Perrin, C.; Sergent, M. *Eur. J. Solid State Inorg. Chem.* **1994**, *31*, 1049.
(10) Cordier, S.; Gulo, F.; Perrin, C. *Solid State Sci.* **1999**, *1*, 637.
(11) Gulo, F.; Perrin, C. *J. Solid State Chem.* **2002**, *163*, 325.
(12) Gulo, F.; Perrin, C. *J. Mater. Chem.* **2000**, *10*, 1721.
(13) (a) Cordier, S.; Perrin, C.; Sergent, M. *Mater. Res. Bull.* **1996**, *31*, 683. (b) Cordier, S.; Perrin, C.; Sergent, M. *Mater. Res. Bull.* **1997**, *32*, 25. (c) Anokhina, E. V.; Essig, M. W.; Lachgar, A. *Angew. Chem., Int. Ed.* **1998**, *37*, 522. (d) Anokhina, E. V.; Day, C. S.; Essig, M. W.; Lachgar, A. *Angew. Chem., Int. Ed.* **2000**, *39*, 1047. (e) Anokhina, E. V.; Day, C. S.; Lachgar, A. *Chem. Commun.* **2000**, 1491. (f) Gulo, F.; Roisnel, T.; Perrin, C. *J. Mater. Chem.* **2001**, *11*, 1237. (g) Anokhina, E. V.; Day, C. S.; Lachgar, A. *Inorg. Chem.* **2001**, *40*, 507. (h) Anokhina, E. V.; Duraisamy, T.; Lachgar, A. *Chem. Mater.* **2002**, *14*, 4111.
(14) Naumov, N. G.; Cordier, S.; Perrin, C. *Angew. Chem., Int. Ed.* **2002**, *41*, 3002.
(15) Naumov, N. G.; Cordier, S.; Gulo, F.; Roisnel, T.; Fedorov, V. E.; Perrin, C. *Inorg. Chim. Acta* **2003**, *350*, 503.
(16) Naumov, N. G.; Virovets, A. V.; Fedorov, V. E. *J. Struct. Chem.* **2000**, *41*, 499.
(17) (a) Schnering, H. G.; Wöhrle, H. *Angew. Chem.* **1963**, *75*, 684. (b) Kepert, D. L. *The Early Transition Metals*; Academic Press: London, 1972. (c) Hillebrecht, H.; Schmidt, P. J.; Rotter, H. W.; Thiele, G.; Zönnchen, P.; Bengel, H.; Cantow, H.-J.; Magonov, S. N.; Whangbo, M.-H. *J. Alloys Compd.* **1997**, *246*, 70.
(18) *Nonius COLLECT, DENZO, SCALEPACK, SORTAV: KappaCCD Program Package*; Nonius B. V.: Delft, The Netherlands, 1999.
(19) Altomare, A.; Burla, M. C.; Camalli, M.; Cascarano, G.; Giacovazzo, C.; Guagliardi, A.; Moliterni, A. G. G.; Polidori, G.; Spagna, R. *J. Appl. Crystallogr.* **1999**, *32*, 115.
(20) Sheldrick, G. M. *SHELXL-97: Program for the Refinement of Crystal Structure*; University of Göttingen: Göttingen, Germany, 1997.

Table 1. Crystal Data and Conditions of Data Collection for $Nb_{10}Cl_{16}O_7$

formula	$Nb_{10}Cl_{16}O_7$
T (K)	298
fw (g/mol)	1608.26
cryst size (mm^3)	$0.12 \times 0.025 \times 0.02$
cryst syst	triclinic
space group	$P\bar{1}$ (No. 2)
a (Å)	6.5140(3)
b (Å)	8.9728(5)
c (Å)	11.3463(6)
α (deg)	77.8032(3)
β (deg)	81.7310(3)
γ (deg)	79.5241(3)
V ($Å^3$)	633.56(6)
Z	1
d_{calcd} (g/cm^3)	4.215
μ (mm^{-1})	6.057
transm range	0.4526 → 0.8246
no. reflns integrated	8029
R_{int}	0.0641
no. indep reflns	2882
no. indep reflns $I > 2\sigma(I)$	1672
θ_{min}; θ_{max}	2.7°; 27.52°
h	−7 → 8
k	−11 → 11
l	−14 → 14
data/restraints/params	2883/2/123
R1[a] ($I > 2\sigma(I)$)	0.0479
wR2 (all data)	0.094
GOF	1.03
($\Delta\rho$) max, min ($e/Å^3$)	1.526, −1.458

[a] $R1 = \sum_{hkl}|F_o - F_c|/\sum_{hkl}|F_o|$; $wR2 = [\sum_{hkl}[w(F_o^2 - F_c^2)^2]/\sum_{hkl}[w(F_o^2)^2]]^{1/2}$.

made up from Nb−Nb pairs with shorter distances than in $NbOCl_2$[17] was also clearly evidenced. However, despite low R values and low residual peaks, this disordered model gave access to average bond lengths that made a rigorous analysis of structural results and comparison to other related compounds difficult. Furthermore, elongated displacement factors, in particular for niobium atoms located in the basal plane of octahedral clusters, left open the question of the possibility of superstructure or hidden lower symmetry. In order to clarify this point, precession images were rebuilt from data collection frames produced by the CCD detector. Then, a careful study of the *hk*0, *hk*1, etc. precession images evidenced very weak diffuse streaks, parallel to *a**, indicating a disorder along the *b* direction. These diffuse scattering lines are located at $k = n/2$ (with n = odd value) indicating that the *b* parameter should be multiplied by 2. Second, the other *hkl* precession images revealed the presence of very weak extra Bragg peaks leading to the loss of the *C*-centered lattice.

Indeed, the data, including weak and very weak spots, were reintegrated on the basis of a triclinic lattice, and the cell parameters were refined as follows: $a = 6.5140(3)$ Å, $b = 8.9728(5)$ Å, $c = 11.3463(6)$ Å, $\alpha = 77.8032(3)°$, $\beta = 81.7310(3)°$, $\gamma = 79.5241(3)°$, $V = 633.56(6)$ $Å^3$. Crystal data and details of the final refinement are given in Table 1. The structure has been solved in the $P\bar{1}$ space group by direct methods (SIR97 program)[19] combined with Fourier difference syntheses and refined against F^2 (SHELXL 97 program).[20] The values of the errors on the supplementary weak and very weak intensities being comparable to the values of the read intensities, the percentage of reflections with $I > 2\sigma(I)$ is lower for this new unit cell than that for the centered monoclinic one. Indeed, the refinement was based on 2882 independent reflections (1672 with $I > 2\sigma(I)$). In contrast to the first structural model, in the present case all the atoms of the structure could be discriminated owing to a lower symmetry. The first sets of refinement evidenced a layered structure with partial occupation of all structural crystallographic sites in relation to two tangled crystallographically independent sheets (sheet 1 and sheet 2) within the layers that are related to each other by a $^1/_2$ *a* translation. For the sake of clarity, a differentiation between the terms layer and sheet will be made in the following. Each layer that will refer to the staking of sheet 1 and sheet 2 within the structure is constituted by one of the two independent sheets related to each other by a $^1/_2$ *a* translation. Subsequently, relevant restraints on atomic displacement parameters were introduced during the refinement in order to discriminate the atoms constituting the two tangled sheets within the layers. This apparent disorder is directly related to staking faults of the layers that frequently occur in layered structures, in particular when the cohesion of the 3D structure is ensured by van der Waals contacts.[17c] No extra symmetry was detected within the layers.

The atomic displacement parameters of the niobium atoms belonging to the clusters within the two sheets were restricted to the same value. Similar restraints were applied for the niobium atoms of the Nb_2 pairs, the Cl atoms belonging to the Nb_6 units, the O atoms belonging to the Nb_6 units, the Cl atoms belonging to the Nb_2 pairs, and the O atoms belonging to the Nb_2 pairs. Beyond the discrimination of all the atomic positions and the anisotropic refinement of all atoms, except the oxygen bridging the Nb_2 pairs, this methodology allowed us to refine the occupancy factors of sheet 1 and sheet 2 to a 70:30 ratio. The final atomic parameters and selected geometrical parameters are reported in Tables 2 and 3, respectively.

EPR Measurements. EPR measurements were made using a Bruker EMX 8/2.7 spectrometer (X-band, $\nu = 9.5$ GHz) equipped with an Oxford Instruments cryogenic unit. No signal corresponding to magnetic clusters or magnetic cations was found.

Resistivity Measurements. Electrical measurements on a compacted pellet were made by a standard four probe configuration using a dc current of 0.1 μA in the temperature range 200−300 K. Single crystals could not be used for this measurement owing to their brittleness. Results indicate a semiconducting behavior.

Theoretical Calculations. Self-consistent ab initio band structure calculations were performed on $Nb_{10}Cl_{16}O_7$ with the scalar relativistic tight-binding linear muffin-tin orbital (LMTO) method in the atomic spheres approximation including the combined correction.[21] Exchange and correlation were treated in the local density approximation using the von Barth−Hedin local exchange correlation potential.[22] Within the LMTO formalism, interatomic spaces were filled with interstitial spheres. The optimal positions and radii of these additional "empty spheres" (ES) were determined by the procedure described in ref 23. There were 41 nonsymmetry-related ES with $0.93 \le r_{ES} \le 1.43$ Å introduced for the calculations. The full LMTO basis set consisted of 5s, 5p, 4d, and 4f functions for Nb spheres, 4s, 3p, and 3d for Cl spheres, 3s, 2p, and 3d functions for O spheres, and s, p, and d functions for ES. The eigenvalue problem was solved using the following minimal basis set obtained from the Löwdin downfolding technique: Nb 5s, 5p, 4d; Cl 3p; O 2p; and interstitial 1s LMTOs. The k space integration was performed using the tetrahedron method.[24] Charge self-consistency

(21) (a) Andersen, O. K. *Phys. Rev. B* **1975**, *12*, 3060. (b) Andersen, O. K. *Europhys. News* **1981**, *12*, 4. (c) Andersen, O. K. In *The Electronic Structure Of Complex Systems*; Phariseau, P., Temmerman, W. M., Eds.; Plenum Publishing Corporation: New York, 1984. (d) Andersen, O. K.; Jepsen, O. *Phys. Rev. Lett.* **1984**, *53*, 2571. (e) Andersen, O. K.; Jepsen, O.; Sob, M. In *Electronic Band Structure and its Application*; Yussouf, M., Ed.; Springer-Verlag: Berlin, 1986. (f) Skriver, H. L. *The LMTO Method*; Springer-Verlag: Berlin, 1984.
(22) von Barth, U.; Hedin, L. *J. Phys. C: Solid State Phys.* **1972**, *5*, 1629.
(23) Jepsen, O.; Andersen, O. K. *Z. Phys. B: Condens. Matter* **1995**, *97*, 35.

Table 2. Atomic Coordinates and Isotropic Displacement Parameters (in Å^2)[a]

atom	Wyckoff	occ	*x*	*y*	*z*	*U*
			Sheet 1			
Nb1	2*i*	0.698(1)	0.1944(3)	0.05172(6)	0.11081(4)	0.0059(1)
Nb2	2*i*	0.698(1)	0.7253(3)	0.05172(6)	0.11081(4)	0.0059(1)
Nb3	2*i*	0.698(1)	−0.0267(2)	0.21116(18)	0.89619(13)	0.0059(1)
Nb5	2*i*	0.698(1)	0.7234(3)	0.3272(2)	0.62914(16)	0.0063(2)
Nb4	2*i*	0.698(1)	0.2988(3)	0.3279(2)	0.62882(15)	0.0063(2)
Cl1	2*i*	0.698(1)	0.5987(14)	−0.1371(6)	0.7496(8)	0.0082(4)
Cl2	2*i*	0.698(1)	0.1001(13)	−0.1428(6)	0.7486(8)	0.0082(4)
Cl4	2*i*	0.698(1)	0.3420(14)	−0.3293(13)	0.9906(9)	0.0082(4)
Cl3	2*i*	0.698(1)	0.1723(14)	0.3270(19)	0.0093(8)	0.0082(4)
Cl5	2*i*	0.698(1)	0.4454(16)	0.4621(12)	0.7462(8)	0.0112(8)
Cl6	2*i*	0.698(1)	−0.0524(17)	0.4634(13)	0.7371(9)	0.0112(8)
Cl7	2*i*	0.698(1)	0.5745(11)	0.1712(6)	0.5274(7)	0.0112(8)
Cl8	2*i*	0.698(1)	1.0681(10)	0.2049(6)	0.5280(6)	0.0112(8)
O2	2*i*	0.698(1)	0.240(2)	0.167(2)	0.783(2)	0.008(1)
O1	2*i*	0.698(1)	0.784(3)	0.166(3)	0.784(2)	0.008(1)
O3	1*d*	0.698(1)	1/2	0	0	0.008(1)
O4	2*i*	0.698(1)	0.7160(17)	0.5011(13)	0.5002(10)	0.0118(18)
			Sheet 2			
Nb21	2*i*	0.302(1)	−0.3072(7)	0.05172(6)	0.11081(4)	0.0059(1)
Nb22	2*i*	0.302(1)	0.2238(8)	0.05172(6)	0.11081(4)	0.0059(1)
Nb23	2*i*	0.302(1)	0.5266(5)	0.7884(4)	0.1042(3)	0.0059(1)
Nb24	2*i*	0.302(1)	0.2018(7)	0.6713(6)	0.3715(4)	0.0063(2)
Nb25	2*i*	0.302(1)	−0.2218(7)	0.6734(6)	0.3700(4)	0.0063(2)
Cl21	2*i*	0.302(1)	−0.086(3)	0.1166(15)	0.258(2)	0.0082(4)
Cl22	2*i*	0.302(1)	0.410(3)	0.1113(15)	0.259(2)	0.0082(4)
Cl23	2*i*	0.302(1)	−0.323(3)	0.320(3)	0.019(2)	0.0082(4)
Cl24	2*i*	0.302(1)	0.845(3)	−0.327(5)	0.9780(18)	0.0082(4)
Cl25	2*i*	0.302(1)	0.046(4)	0.520(3)	0.272(2)	0.0112(8)
Cl26	2*i*	0.302(1)	0.549(4)	0.517(3)	0.2663(18)	0.0112(8)
Cl27	2*i*	0.302(1)	−0.071(3)	0.8338(16)	0.4674(16)	0.0112(8)
Cl28	2*i*	0.302(1)	−0.571(3)	0.7923(17)	0.4778(17)	0.0112(8)
O21	2*i*	0.302(1)	−0.285(6)	0.846(6)	0.210(5)	0.008(1)
O22	2*i*	0.302(1)	0.251(7)	0.846(6)	0.210(5)	0.008(1)
O23	1*a*	0.302(1)	0	0	0	0.008(1)
O24	2*i*	0.302(1)	−0.218(4)	0.505(3)	0.500(2)	0.0118(18)

[a] Sheet 1 is related to sheet 2 by $^1/_2$ *a* translation.

and the average properties were obtained from 255 irreducible *k* points. A measure of the magnitude of the bonding was obtained by computing the crystal orbital Hamiltonian populations (COHP) which are the Hamiltonian population weighted density of states (DOS).[25,26] As recommended, a reduced basis set (in which all ES LMTOs have been downfolded) was used for the COHP calculations.[27] Bands, DOS, and COHP curves were shifted so that ϵ_F lies at 0 eV.

Results

Description of the Structure. The apparent disorder of the structure is related to stacking faults and must not be attributed to any difference of electronic or physicostructural properties between the two independent sheets. The structural analysis reveals that the interatomic distances of the first sheet (sheet 1, occupation factor = 0.7) are quite similar, within the su's, to those observed in the second sheet (sheet 2, occupation factor = 0.3). Let us recall that the calculated su's on the interatomic distances take into account, as a weighting factor, the occupation factor of each sheet. Consequently, the calculated su's on the interatomic distances are 2.33 lower in the first sheet (occupation factor = 0.7) than those of the second sheet (occupation factor = 0.3). In the following discussion, we will consider the interatomic distances observed in sheet 1 that are more relevant because of their higher accuracy.

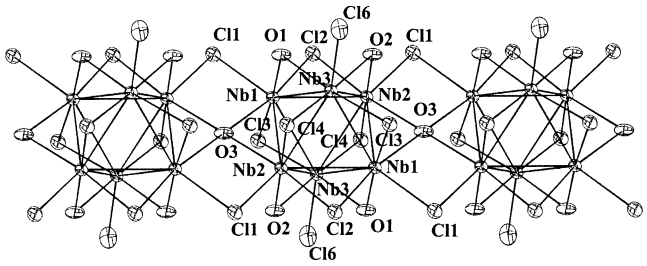

Figure 1. Representation of the interconnected $Nb_6Cl^i_6O^i_6Cl^a_6$ cluster units in the $[Nb_6Cl^i_6O^i_4O^{i-i}_{2/2}Cl^{a-a}_{4/2}Cl^a_2]_\infty$ infinite chains. Displacement ellipsoids are shown at the 90% probability level.

Description of the $Nb_6Cl^i_6O^i_6Cl^a_6$ Cluster Unit. The Nb_6 cluster that is edge-bridged by six inner oxygen and six inner chlorine ligands (Figure 1) exhibits the same oxygen/chlorine ordered distribution around the octahedral Nb_6 cluster as that found for $PbLu_3Nb_6Cl_{15}O_6$.[13f] In the title compound, the six crystallographically independent Nb−Nb bond lengths spread within the range 2.788(2)−3.056(3) Å (av 2.898(2) Å). They compare rather well with the 2.7900(8) and 3.0173(9) Å (av 2.903(1) Å) Nb−Nb bond lengths found in $PbLu_3Nb_6Cl_{15}O_6$. The average Nb−Nb bond length in the title compound is also similar to Nb−Nb distances measured in other Nb_6 oxychlorides having six inner oxygen atoms and a VEC value

(24) Blöchl, P. E.; Jepsen, O.; Andersen, O. K. *Phys. Rev. B* **1994**, *49*, 16223.
(25) Dronskowski, R.; Blöchl, P. E. *J. Phys. Chem.* **1993**, *97*, 8617.
(26) Boucher, F.; Rousseau, R. *Inorg. Chem.* **1998**, *37*, 2351.
(27) Jepsen, O.; Andersen, O. K. Personal communication.

Table 3. Selected Interatomic Distances (Å) in $Nb_{10}Cl_{16}O_7$

sheet 1		sheet 2	
	Nb_6 Cluster Unit		
Nb1−Nb2	2.809(1)	Nb21−Nb22	2.809(1)
Nb1−Nb2	3.056(3)	Nb21−Nb22	3.055(7)
Nb1−Nb3	2.794(2)	Nb21−Nb23	2.791(5)
Nb1−Nb3	2.973(2)	Nb21−Nb23	2.972(4)
Nb2−Nb3	2.788(2)	Nb22−Nb23	2.796(4)
Nb2−Nb3	2.970(2)	Nb22−Nb23	2.980(4)
Nb1−Cl1	2.533(10)	Nb21−Cl21	2.571(23)
Nb1−Cl2	2.448(8)	Nb21−Cl22	2.374(20)
Nb1−Cl3	2.483(15)	Nb21−Cl23	2.402(25)
Nb1−O1	2.055(24)	Nb21−O21	1.941(49)
Nb1−O3	2.225(2)	Nb21−O23	2.233(4)
Nb2−Cl1	2.552(8)	Nb22−Cl21	2.493(20)
Nb2−Cl2	2.432(10)	Nb22−Cl22	2.405(24)
Nb2−Cl4	2.501(11)	Nb22−Cl24	2.448(40)
Nb2−O2	2.067(17)	Nb22−O22	1.919(49)
Nb2−O3	2.230(2)	Nb22−O23	2.223(4)
Nb3−Cl3	2.437(14)	Nb23−Cl23	2.497(27)
Nb3−Cl4	2.453(9)	Nb23−Cl24	2.533(24)
Nb3−Cl6	2.575(10)	Nb23−Cl26	2.718(23)
Nb3−O1	2.039(25)	Nb23−O21	2.032(57)
Nb3−O2	2.037(16)	Nb23−O22	2.064(46)
	Niobium Pair Unit		
Nb4−Nb5	2.765(3)	Nb24−Nb25	2.758(7)
Nb4−Cl5	2.366(12)	Nb24−Cl25	2.372(30)
Nb4−Cl6	2.652(10)	Nb24−Cl26	2.691(24)
Nb4−Cl7	2.387(7)	Nb24−Cl27	2.375(17)
Nb4−Cl8	2.533(8)	Nb24−Cl28	2.545(22)
Nb4−O2	2.057(19)	Nb24−O22	2.188(50)
Nb4−O4	1.883(10)	Nb24−O24	1.910(23)
Nb5−Cl5	2.387(10)	Nb25−Cl25	2.322(24)
Nb5−Cl6	2.631(13)	Nb25−Cl26	2.747(30)
Nb5−Cl7	2.394(8)	Nb25−Cl27	2.399(21)
Nb5−Cl8	2.541(6)	Nb25−Cl28	2.584(18)
Nb5−O1	2.062(22)	Nb25−O21	2.158(50)
Nb5−O4	1.899(10)	Nb25−O24	1.875(23)

of 14.[15] This structural result suggests at first sight that the VEC value is equal to 14, although the absence of countercations and the interconnections between Nb_6 clusters and Nb_2 entities make difficult the calculation of the VEC. The Nb−Cl and Nb−O bond lengths are similar to the corresponding ones in other Nb_6 oxychlorides.[9−13] The $Nb_6Cl^i{}_6O^i{}_6Cl^a{}_6$ units are linked to each other along the *a* direction by shared inner oxygen and apical chlorine atoms to form $[Nb_6Cl^i{}_6O^i{}_4O^{i-i}{}_{2/2}Cl^{a-a}{}_{4/2}Cl^a{}_2]_\infty$ infinite chains. Such a connectivity was previously encountered in niobium oxoniobates with the general formula MNb_8O_{14} (M = K, Ba, La)[28] but was never encountered hitherto in Nb_6 oxychlorides. Let us note that in both compounds the O^{i-i} bridging ligand is located in an unusual site built up from a quasiregular niobium square plane.

Description of the $Nb_2(\mu_2\text{-}Cl^i)_2Cl^a{}_4O_4$ Unit. The $Nb_2(\mu_2\text{-}Cl^i)_2Cl^a{}_4O_4$ unit (Figure 2) can be described as two edge-shared NbO_2Cl_4 distorted octahedra with the two oxygen atoms in *trans* position resulting in the occurrence of Nb−Nb···Nb alternation with short and long Nb−Nb interatomic distances (2.765 and 3.749 Å). The $Nb_2(\mu_2\text{-}Cl)_2Cl_4O_4$ units are linked to each other via four Cl and two O outer ligands to form $[\{Nb_2(\mu_2\text{-}Cl)_2O_{2/2}Cl_{4/2}O_2\}_2]_\infty$ double chains. This structural part can be compared to that of $NbOCl_2$.[17] However, instead of double chains, the structure

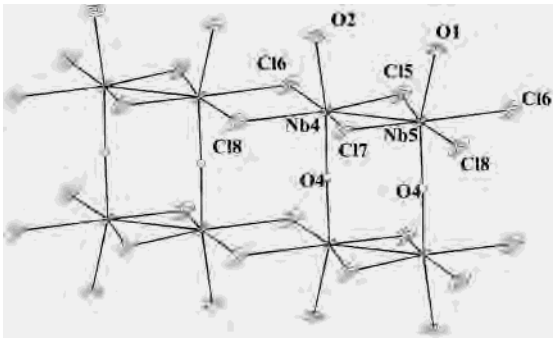

Figure 2. Representation of the interconnected $Nb_2(\mu_2\text{-}Cl)_2Cl_4O_4$ units in the $[\{Nb_2(\mu_2\text{-}Cl)_2O_{2/2}Cl_{4/2}O_2\}_2]_\infty$ double chains. Displacement ellipsoids are shown at the 90% probability level. O4 has been refined isotropically.

of the latter is based on $[Nb_2(\mu_2\text{-}Cl)_2O_{2/2}Cl_{4/2}O_{2/2}]_\infty$ layers. The structural models obtained for $NbOCl_2$ that exhibit also a layered structure led to erroneous interatomic distances.[2,17a,b] New investigations of this structure evidenced Nb−Nb pairs with a bond length equal to 2.97 Å, Nb−O interatomic distances ranging from 1.92 to 2.02 Å and Nb−Cl distances ranging from 2.43 to 2.50 Å.[17c] The Nb−Cl and Nb−O interatomic distances are quite similar in the title compound and in $NbOCl_2$. Tight-binding band calculations performed on $NbOCl_2$ revealed that the out-of-plane Nb displacement is a crucial key in explaining the semiconducting properties of this material.[29] As observed in $NbCl_4$, the niobium atoms are not displaced out of the Cl_4 plane in $Nb_{10}Cl_{16}O_7$. The shorter Nb−Nb bond lengths within the Nb_2 pairs in $Nb_{10}Cl_{16}O_7$ compared to those observed in $NbOCl_2$ and $NbCl_4$ seem to indicate that a larger number of electrons might be involved in the Nb−Nb bonding of the infinite Nb_2 chains.

Description of the Resulting Structure. The four remaining O^i atoms and the two remaining Cl^a atoms of the $[Nb_6Cl^i{}_6O^i{}_4O^{i-i}{}_{2/2}Cl^{a-a}{}_{4/2}Cl^a{}_2]$ cluster chains are shared with the four remaining oxygen atoms of the $[\{Nb_4(\mu_2\text{-}Cl)_4O_{4/2}\text{-}Cl_{8/2}O_4\}]_\infty$ double chains and one-half of chlorine ligand involved in the connection of the $Nb_2(\mu_2\text{-}Cl)_2Cl_4O_4$ units in the $[(Nb_4(\mu_2\text{-}Cl)_4O_{4/2}Cl_{8/2}O_4)]_\infty$ double chains. The resulting $Nb_{10}Cl_{16}O_7$ layers (Figure 3), that can be written as $Nb_6Cl^i{}_6O^i{}_{4/2}O^{i-i}{}_{2/2}Cl^{a-a}{}_{4/2}Cl^a{}_{2/2}Nb_4(\mu_2\text{-}Cl)_4O_{4/2}Cl_{4/2}Cl_{4/4}O_{4/2}$, are parallel to the *bc* plane. The cohesion of the structure is ensured by van der Waals contacts between chlorine atoms of adjacent layers, which is one of the proposed criteria for layered structure.[31]

Staking Description. The layers are stacked along the [011] direction. Such a stacking can schematically be described as an ABA succession of layers if one considers an ordered structure. The projections of the stacking along the *a* and the [110] directions are represented in Figures 4 and 5, respectively. As proposed in the case of $NbOCl_2$,[17d] for every alternating A and B layers, two positions of the sheets that are related to each other by a 1/2 *a* translation are possible. For clarity, we will label them A1, A2 and B1, B2. Indeed, regardless of the A and B type of layer staking (type 1, A1B1A1) or (type 2, A2B2A2), the projection along the *a* direction remains unchanged. However, the structural

(28) Köhler, J.; Tichtau, R.; Simon, A. *J. Chem. Soc., Dalton Trans*. **1991**, 829.

(29) Whangbo, M. H. *Inorg. Chem*. **1982**, *21*, 1721.

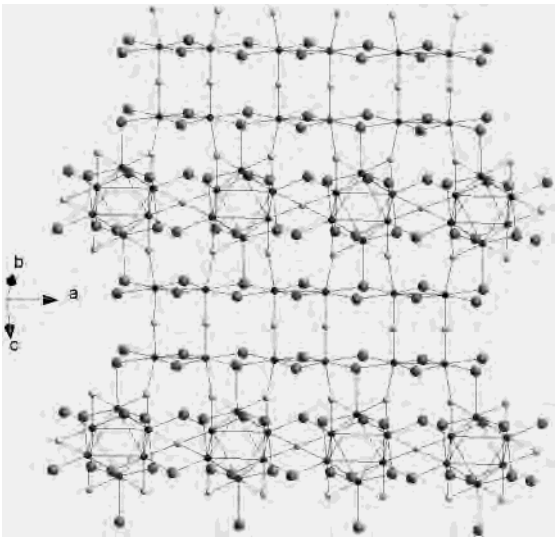

Figure 3. Representation of the resulting $Nb_{10}Cl_{16}O_7$ layer that spreads along the *a* direction.

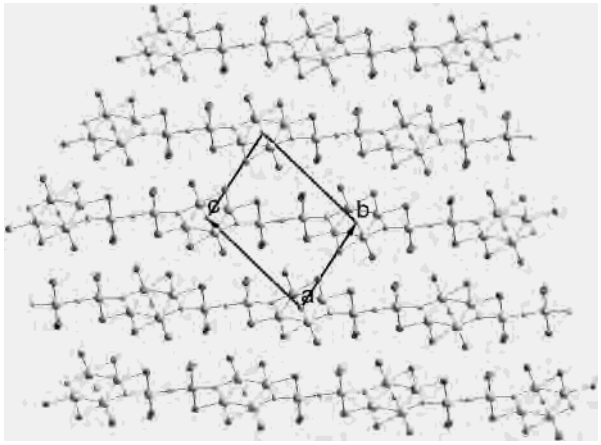

Figure 4. Projection of the structure along the [100] direction.

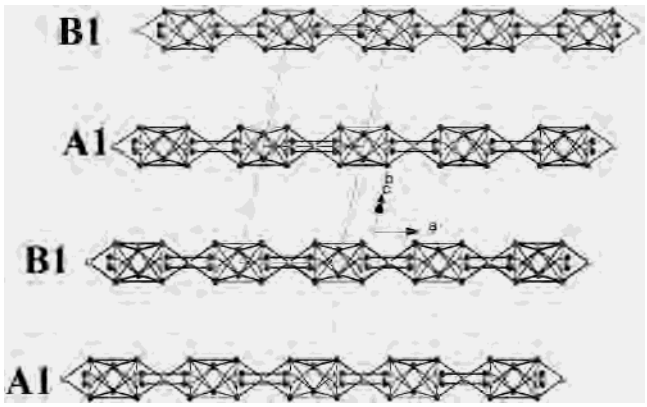

Figure 5. A1B1A1 succession of layers along the [110] direction. For sake of clarity, the chlorine atoms are not represented.

results show a type 1/type 2 random stacking along the [011] direction with a 70:30 ratio. This disorder can be modeled according to a simple mathematical combination: for 10 successive layers, seven of them are stacked according to type 1 and the three other ones according to type 2; the number of possible (type 1)/(type 2) combinations being equal to 120 (10!/(7! × 3!)). For illustration, a A1B1A2A1 disordered sequence is represented in Figure 6.

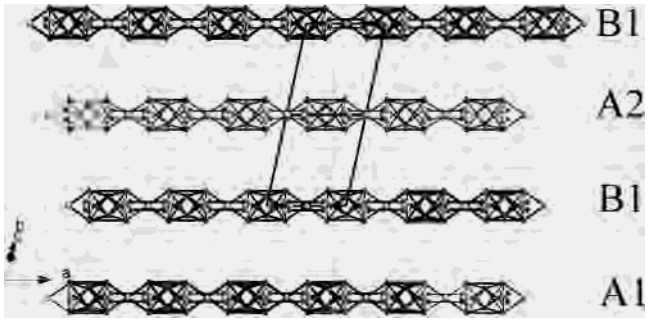

Figure 6. Example of stacking fault in $Nb_{10}Cl_{16}O_7$ with a B1A2B1 sequence instead of B1A1B1. For sake of clarity, the chlorine atoms are not represented.

Table 4. Closest Cl−Cl Interatomic Distances between Layers (Å) Corresponding to van der Waals Contacts

A1B1A1 ordered stacking		A1B2A1 disordered stacking	
	Nb_6 Cluster Unit/Nb_2 Cluster Unit		
Cl3−Cl6	3.679	Cl4−Cl26	3.589
Cl4−Cl5	3.584	Cl3−Cl25	3.677
Cl1−Cl7	3.577	Cl1−Cl27	3.622
Cl1−Cl8	3.656	Cl1−Cl28	3.632
Cl2−Cl8	3.648	Cl2−Cl28	3.575
Cl2−Cl7	3.549	Cl2−Cl27	3.586
	Nb_2 Pair Units/Nb_2 Pair Units		
Cl7/Cl7	3.582	Cl7−Cl27	3.583
	Nb_6 Cluster Unit/Nb_6 Cluster Unit		
Cl3−Cl4	3.417	Cl3−Cl23	3.422
Cl3−Cl3	3.471	Cl3−Cl24	3.414
Cl4−Cl4	3.350	Cl4−Cl23	3.471
Cl4−Cl3	3.417	Cl4−Cl24	3.449

Structural Cohesion. The cohesion of the $Nb_{10}Cl_{16}O_7$ structure is ensured by three types of van der Waals contacts between layers: Nb_2 unit/Nb_2 unit, Nb_2 unit/Nb_6 cluster unit, and Nb_6 cluster unit/Nb_6 cluster unit. In Table 4 are reported the closest Cl−Cl interatomic distances between layers corresponding to van der Waals contacts (i.e., ca. 3.5 Å).[32] The analysis of these data indicates two features: (i) the strongest interactions are found between niobium cluster units and between niobium pair units, (ii) the Cl−Cl interatomic distances remain unchanged for the A1B1A1 succession of layers compared to the A1B2A1 one (and obviously for the homologous sequences B1A2B1 as well as for the less probable but theoretically possible A2B1A2 and B2A1B2 sequences). The latter point which has not been discussed yet in the case of $NbOCl_2$ appears to be the reason for the disordered stacking of layers. The absence of "driving forces" during the crystallization process, such as countercations that would impose a particular coordinence with their specific environment, leads to a random stacking.

$Nb_{10}Cl_{16}O_7$ crystals are brittle similarly to the two homologous $Mo_6I_8S_2$[34] and Nb_6I_9S.[35] These thio-iodides are

(30) Taylor, D. R.; Calabrese, J. C.; Larsen, E. M. *Inorg. Chem.* **1977**, *16*, 721.
(31) Hulliger, F. *Structural Chemistry of Layer-Type Phases*; Reidel: Dordrecht, 1976; p 28.
(32) Bondi, A. *J. Phys. Chem.* **1964**, *68*, 441.
(33) Schäfer, H.; von Schnering, H. G.; Tillack, J.; Kuhnen, F.; Wöhrle, H.; Baumann, H. *Z. Anorg. Allg. Chem.* **1967**, *353*, 281.
(34) Perrin, C.; Sergent, M. *J. Chem. Res.* **1983**, *2*, 38.
(35) Meyer, H.-J.; Corbett, J. D. *Inorg. Chem.* **1991**, *30*, 963.

built up from infinite $[Mo_6I^i_5S^iS^{i-i}_{2/2}I^{a-a}_{6/2}]$ and $[Nb_6I^i_6S^iS^{i-i}_{2/2}I^{a-a}_{6/2}]$ chains, respectively, in which all apical iodine atoms are shared between units. Only van de Waals contacts exist between adjacent chains. On the contrary, crystals of molybdenum and tungsten M_6X_{12} binary halides are quite stable under handling. Their structure is characterized by $M_6X^i_8X^{a-a}_{4/2}X^a_2$ layers, and the structural cohesion is also ensured by van der Waals contacts between layers, but an unshared apical ligand leads to strongly interpenetrated layers.[33] This unshared apical ligand appears to be crucial to prevent the sliding of layers with respect to each other.

Theoretical Considerations. Many theoretical studies have been devoted to the octahedral cluster compounds of general formula $[(M_6X^i_{12})L^a_6]^{n-}$ (M = Nb, Ta; X^i = two-bonded inner halide ligand; L^a = two-electron donor apical ligand (H_2O, OH^-, Cl^-, Br^-)).[36] With the aid of symmetry and orbital overlap arguments,[36] the MO pattern of this type of cluster can be determined by considering the interaction of the frontier orbitals of six square-pyramidal ML_5 fragments since each transition metal atom is locally surrounded by four inner and one apical ligands. Considering the O_h symmetry, a set of 8 metal−metal bonding MOs of symmetry a_{1g}, t_{2g}, t_{1u}, and a_{2u} and 16 metal−metal antibonding MOs is expected for this kind of $M_6X^i_{12}L^a_6$ octahedral unit. The complete occupation of the M−M bonding MOs fulfills a closed-shell configuration with a VEC of 16.[36] However, owing to the M−X and M−L antibonding character of the highest M−M bonding a_{2u} level that lies in the middle of a large energy gap separating the other seven M−M bonding MOs from M−M antibonding MOs, vacancy (14 VEs) or partial occupation (15 VEs) of this overall nonbonding MO can be favored. Indeed, oxychloride cluster compounds bonded to three or more oxide inner ligands have a VEC of 14.[8−11] Such an electron count for the $Nb_6Cl^i_6O^i_6Cl^a_6$ cluster belonging to the title compound leaves an average electron count of 1.5 on each metal atom of the $[\{Nb_2(\mu_2\text{-}Cl)_2O_{2/2}Cl_{4/2}O_2\}_2]_\infty$ double chains. This is more than the d^1 electron count of metal atoms in the related $NbOCl_2$ compound that contains similar $(Nb_2(\mu_2\text{-}Cl^i)_2Cl^a_4O_4$ units with an alternation of two unequal Nb−Nb distances.[17,29] In order to confirm the electron distribution of 14 electrons for octahedral cluster and $d^{1.5}$ on the metal atoms of the Nb_2 pairs, periodic calculations using density functional theory were carried out on models of $Nb_{10}Cl_{16}O_7$ made up from sheet 1 or sheet 2. Similar results were obtained for both models, but we will only report the results obtained for the model based on sheet 1. Density of states (DOS) and crystal orbital Hamiltonian population (COHP) curves are sketched in Figure 7. A first analysis reveals that the Nb−Nb COHP curve corresponding to the Nb−Nb contacts of the octahedral cluster shows that Nb−Nb bonding bands deriving from the a_{2u} molecular level above the Fermi level are vacant. This confirms the electron count of 14 for the octahedral $Nb_6Cl^i_6O^i_6Cl^a_6$ unit. The Fermi level lies above a peak that shows a major character of niobium atoms of the Nb_2 pairs (Figure 7c). This peak of DOS is Nb−Nb bonding in character. The following peak

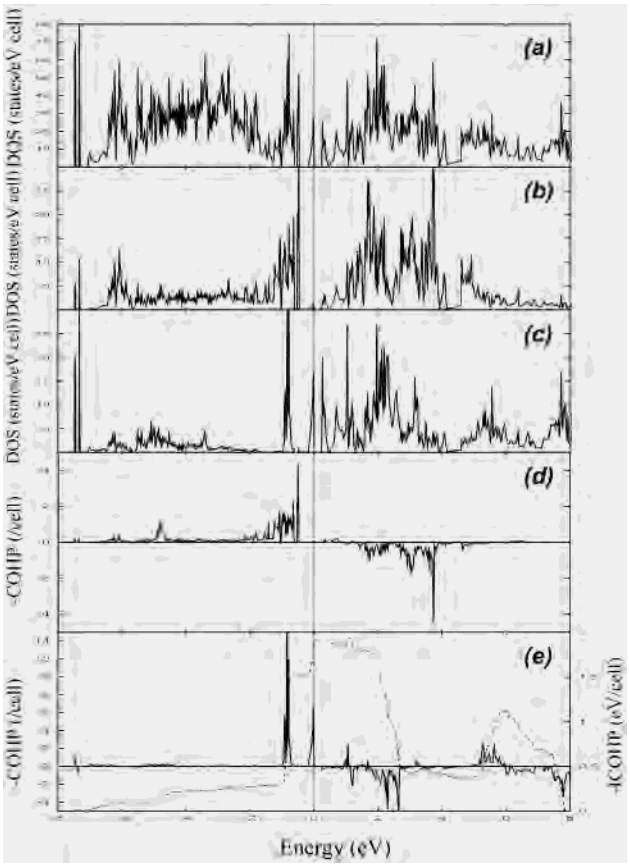

Figure 7. LMTO calculations for $Nb_{10}Cl_{16}O_7$: (a) total DOS, (b) $Nb_6O^i_6Cl^i_6Cl^a_6$ projected DOS, (c) $[\{Nb_2(\mu_2\text{-}Cl)_2O_{2/2}Cl_{4/2}O_2\}_2]_\infty$ double chains projected DOS, (d) Nb−Nb COHP curve for $Nb_6O^i_6Cl^i_6Cl^a_6$ cluster unit, and (e) Nb−Nb COHP curve for $[\{Nb_2(\mu_2\text{-}Cl)_2O_{2/2}Cl_{4/2}O_2\}_2]_\infty$ double chains. The integrated COHP is shown as a dashed line.

of DOS lying around −1 eV shows a stronger Nb−Nb bonding character in the chains as well (Figure 7e). Previous theoretical studies on $NbOCl_2$[29] indicate that the latter peak around −1 eV is σ-type bonding whereas the former, just below 0 eV, is π-type bonding. In the case of $NbOCl_2$ which contains d^1 metal, only the lowest band is filled. In the case of $Nb_{10}Cl_{16}O_7$, DOS and COHP curves show that the π-type Nb−Nb bonding band is also occupied. This explains the very short Nb−Nb distance of 2.765 Å in the title compound compared to the corresponding separations in $NbCl_4$[30,37] and $NbOCl_2$[17,29] (3.029[30] and 2.97[17c] Å, respectively). The 0.33 eV computed band gap is consistent with semiconducting behavior as suggested by the transport property measurements.

Concluding Remark. This work reports the synthesis, the single crystal structure determination, and the electronic structure of a novel layered $Nb_{10}Cl_{16}O_7$ oxychloride compound, built up from both Nb_2 pairs and Nb_6 octahedral clusters. DFT results suggest, in agreement with the structural results, that, among the 20 metallic electrons involved in the metal−metal bonding of $Nb_{10}Cl_{16}O_7$, 14 electrons belong to the octahedral $Nb_6Cl^i_6O^i_6Cl^a_6$ unit whereas the 6 others (i.e., 1.5 per Nb atom) participate to the bonding in the distorted $[\{Nb_2(\mu_2\text{-}Cl)_2O_{2/2}Cl_{4/2}O_2\}_2]_\infty$ double chains.

(36) Ogliaro, F.; Cordier, S.; Halet, J.-F.; Perrin, C.; Saillard, J.-Y.; Sergent, M. *Inorg. Chem.* **1998**, *37*, 6199 and references therein.

(37) Whangbo, M.-H.; Foshee, M. J. *Inorg. Chem.* **1981**, *20*, 113.

Acknowledgment. We thank T. Guizouarn (Rennes) for resistivity measuments, J.-Y. Thépot (Rennes) for EPR measurements, and J.-C. Jegaden (Rennes) for EDS analysis. S.C. and C.P. are grateful to "Fondation Langlois" for financial support.

Supporting Information Available: Two X-ray crystallographic information files of the structure of $Nb_{10}Cl_{16}O_7$ solved in $C2/m$ and $P\bar{1}$ space groups, respectively (CIF). This material is available free of charge via the Internet at http://pubs.acs.org.

IC0350990